Drug Metabolism and Pharmacokinetics 56 (2024) 101005

Contents lists available at ScienceDirect

Drug Metabolism and Pharmacokinetics

journal homepage: www.journals.elsevier.com/drug-metabolism-and-pharmacokinetics

Regular Article

In vitro demonstration of antedrug mechanism of a pharmacokinetic booster to improve CYP3A4 substrates by CYP3A4-mediated metabolism inhibition

Makoto Kataoka *, Sae Takenaka, Shota Fujii, Takato Masada, Keiko Minami, Toshihide Takagi, Masaaki Omote, Kentaro Kawai **, Shinji Yamashita

Faculty of Pharmaceutical Sciences, Setsunan University, 45-1 Nagaotoge-cho, Hirakata, Osaka, 573-0101, Japan

ARTICLE INFO

Keywords:
Booster
CYP3A4
Drug-drug interaction
Inhibition
Metabolism

ABSTRACT

We previously reported novel benzyl-ether derivatives with an imidazole ring and a hydroxyl group (A-01) or carboxyl group (B-01) and esters (2 esters of A-01, and 7 esters of B-01) as pharmacokinetics (PK) boosters. This study demonstrates how these ester compounds embody the concept of a safe pharmacokinetic booster, with potent and transient inhibition of CYP3A4-mediated drug metabolism. As a model CYP3A4 substrate and CYP3A4 enzyme, midazolam (MDZ) and rat liver microsomes were used. A-01 inhibited MDZ metabolism significantly, while B-01 induced only slight inhibition. Although rat liver microsomes hydrolyzed the ester compounds over time, several ester compounds strongly inhibited MDZ metabolism. Due to the significant activity of A-01, A-01 esters affected MDZ metabolism, irrespective of hydrolysis state. Time-dependent inhibition evaluation indicated that the B-01 ester inhibition is not mechanism-based, as hydrolysis eliminated MDZ metabolism inhibition. We report that the B-01 esters significantly inhibit CYP3A4-mediated drug metabolism, and upon hydrolysis this property is eliminated. In conclusion, B-01 ester compounds may be safe PK boosters with antedrug characteristics.

1. Introduction

Over the past few decades, the major reason for discontinuing oral dosage form drug development has changed [1]. Previously, drug candidates mostly showed poor pharmacokinetics (PK), such as poor metabolic stability and poor oral absorption, which limited the development of these drugs. This limitation has changed over time, shifting from poor PK to problems of marketing, manufacturing cost, safety, and so on. Rapid drug metabolism during absorption may not only cause poor oral availability but may also induce severe side effects through drug-drug interactions (DDIs). PK research has greatly improved drug development, but the true potential of many drug candidates is not yet achieved.

To overcome poor PK due to drug metabolism after oral administration, several PK boosters, specifically enzyme inhibitors, are used to improve the oral availability of drugs with poor PK. For instance, carbidopa is administered with L-dopa to prevent L-dopa degradation by decarboxylase in plasma [2]. Furthermore, clavulanic acid inhibits β-lactamase, improving the oral availability of β-lactam antibacterial agents [3]. These inhibitory effects are highly specific, thus DDIs are unlikely. However, developing specific inhibitors is time-consuming and costly. Therefore, non-specific inhibitors of enzyme-mediated metabolism may improve systemic exposure to drugs.

Ritonavir strongly inhibits CYP3A4-mediated metabolism and P-gp-mediated efflux [4,5]. It is co-prescribed to increase the plasma concentration of protease inhibitors saquinavir and lopinavir, for effective HIV/AIDS treatment [6–9]. Recently, ritonavir was also dosed with nirmatrelvir to enhance nirmatrelvir oral availability by inhibiting CYP3A4-mediated metabolism [10,11]. As ritonavir induces several CYPs and UGTs [12,13], many drugs, such as CYPs, UGTs, or P-gp substrates except for anti-HIV agents and nirmatrelvir, are contra-indicated upon ritonavir prescription to prevent severe adverse effects. Cobicistat was developed to replace ritonavir [14,15] as it strongly inhibits CYP-mediated metabolism but does not induce CYPs, UGTs, and P-gp [16]. However, cobicistat has similar contra-indications as ritonavir. Hence, non-specific boosters, such as ritonavir and cobicistat, have significant useful effects on the PK profile of CYP3A4 substrates, but are limited by restriction of co-administration with other

* Corresponding author.
** Corresponding author.
E-mail addresses: makoto@pharm.setsunan.ac.jp (M. Kataoka), kentaro.kawai@pharm.setsunan.ac.jp (K. Kawai).

https://doi.org/10.1016/j.dmpk.2024.101005
Received 14 November 2023; Received in revised form 18 January 2024; Accepted 20 February 2024
Available online 2 March 2024

CYP3A4 substrates.

In terms of safety, the following properties are ideal for a PK booster that enhances the oral availability of CYP3A4 substrates.

(1) Potent inhibition of CYP3A4-mediated drug metabolism
(2) Rapid and transient effect
(3) No additional pharmaceutical effects, toxicity, or protein expression induction

To achieve this, we synthesized novel benzyl-ether derivatives incorporating an imidazole and ester bond [17]. The previous study primarily focused on compound synthesis and inhibitory effect evaluation. In this study, *in vitro* studies were performed to evaluate the above-mentioned first and second ideal PK booster characteristics to demonstrate potentials as novel and safe PK boosters with antedrug characteristics.

2. Materials and methods

2.1. Materials

1-Aminobenzotriazole (ABT), irinotecan hydrochloride (IRT), itraconazole (ITZ), ketoconazole (KTZ), and temocapril (TEM) were purchased from Tokyo Chemical Industry Co., Ltd. (Tokyo, Japan). Midazolam (MDZ) was obtained from Wako Pure Chemicals (Osaka, Japan). β-Nicotinamide adenine dinucleotide 2′-phosphate reduced

Table 1
Structures, molecular weights, and ionization conditions of all compounds used in this study.

Compound	Structure	Molecular weight	*m/z* (+)		Cone voltage (V)	Collision energy (eV)
			Parent ion	Daughter ion		
Midazolam (MDZ)		325.77	327.08	292.12	30	30
1-Aminobenzotriazole (ABT)		134.14	134.88	79.93	50	18
Itraconazole (ITZ)	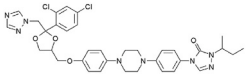	705.63	706.29	146.07	50	50
Ketoconazole (KTZ)	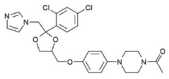	531.43	532.34	81.77	50	40
A-01	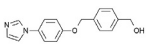	280.32	281.11	159.86	40	20
A-02	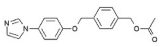	322.36	323.13	159.90	40	30
A-03	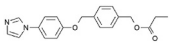	336.38	337.13	159.87	30	30
B-01	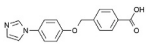	294.30	295.07	159.87	40	20
B-02	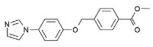	308.33	309.11	159.87	40	20
B-03	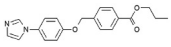	336.38	337.11	159.84	50	20
B-04	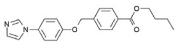	350.41	351.15	159.85	20	20
B-05	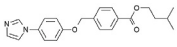	364.44	365.18	159.82	30	30
B-06	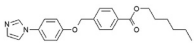	378.46	379.17	159.87	50	30
B-07	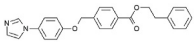	398.45	399.14	159.85	40	30
B-08	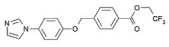	376.33	377.08	159.87	50	30
Irinotecan (IRT)	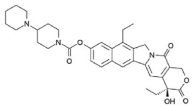	586.68	587.66	190.14	40	40
Temocapril (TEM)	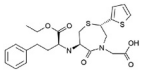	576.57	587.66	167.22	50	40

tetrasodium salt hydrate (NADPH) was purchased from Oriental Yeast Co., Ltd. (Tokyo, Japan). Male SD rat liver microsomes (20 mg protein/mL) were obtained from Sekisui Medical Co. Ltd (Tokyo, Japan). All test compounds shown in Table 1 used in this study were synthesized in-house for the previous study [17].

2.2. Metabolism study

2.2.1. Inhibition study

The metabolism of MDZ was examined using male SD rat liver microsomes, with and without potential PK booster compounds. The buffer solution consisted of 100 mM potassium phosphate buffer with 3.3 mM $MgCl_2$ (pH 7.4). The reaction solution (450 μL) containing 0.02 mg protein of microsomes, 1.11 μM MDZ (final conc.: 1 μM), and with or without 11.1 μM of ABT, ITZ, KTZ, or each compound in groups A and B (final conc.: 10 μM) in the buffer was pre-incubated at 37 °C for 10 min. Fifty microliters of the solution containing 20 mM of NADPH in the buffer were added to the pre-incubated reaction solution. Then, 50 μL of the reaction solution was sampled and immediately mixed with 450 μL of acetonitrile at 0, 2, 5, 10, and 30 min. The mixtures were shaken, and supernatants collected after centrifugation at approximately 20,000 g and 4 °C for 10 min (Model 6200, KUBOTA, Tokyo, Japan). The supernatants were analyzed by LC-MS/MS (see section 2.3.).

2.2.2. Hydrolysis study

To evaluate hydrolysis, a hydrolysis buffer of 50 mM HEPES buffer (pH 7.4) was used. Stock solutions of compounds (10 mM) prepared with dimethyl sulfoxide were diluted to one hundredth with the buffer. The reaction solution (450 μL) containing 0.02 mg protein of microsomes in buffer was pre-incubated at 37 °C for 10 min. Degradation was initiated by adding 50 μL of each compound solution (final conc.: 10 μM). The same sampling and sample treatment procedure as the inhibition study was used.

2.2.3. Time-dependent inhibition study

Time-dependent inhibition was performed as follows. The reaction solution (400 μL) containing 0.02 mg protein of microsomes, with or without 12.5 μM of each compound in the buffer was pre-incubated at 37 °C for 10 min. Fifty microliters of the solution containing 10 mM of NADPH in the buffer were added to the pre-incubated reaction solution. After 30 min of reaction without MDZ, 50 μL of the solution containing MDZ (10 μM) and NADPH (20 mM) in buffer was added to the reaction solution to initiate the time-dependent inhibition. The same sampling and sample treatment procedure as the inhibition study was used.

2.3. Analytical method

The amount of each compound in the supernatant was measured by UPLC (ACQUITY® UPLC, Waters, MA) equipped with a tandem mass spectrometer (ACQUITY® TQD, Waters). A reverse-phase Waters Acquity® UPLC BEH C18 analytical column (Waters, 50 × 2.1 mm I.D., 1.7-μm particle size) was used with a mobile phase gradient of 0.1% (v/v) formic acid in water and acetonitrile containing 0.1% (v/v) formic acid at 40 °C. An injection volume of 10 μL was used for all samples. Ionization conditions for the analysis of each compound were as follows: electrospray ionization, positive mode; source temperature, 150 °C; desolvation temperature, 400 °C. Other conditions for each compound are listed in Table 1.

2.4. Calculation of metabolic ratio and inhibition ratio

Metabolic rate for each compound were evaluated using the amount of compound eliminated with a 10 min incubation period and the following equation:

Metabolic rate (pmol/min/mg protein)= (initial amount - remaining amount)/incubation time/amount of the protein (Eq. 1)

where the initial amount is 500 pmol, the remaining amount is obtained by LC-MS/MS quantification of samples, incubation time is 10 min, and the amount of protein is 0.02 mg. The metabolic ratio (%) was calculated by the ratio of metabolic rate with inhibitor to the metabolic rate without inhibitor (control). The inhibition ratio (%) was obtained by subtracting the metabolic ratio from 100%.

2.5. Statistical analysis

All data are presented as means with standard deviation (s.d.) for individual groups. Significance was assessed by one-way analysis of variance using Dunnett's test (JMP Pro, 15.1.0, SAS Institute Inc., Cary, NC) with p values of 0.05 or less considered significant.

3. Results

3.1. Effect of ABT, ITZ, and KTZ on MDZ metabolism and their degradations

The time profiles of MDZ metabolism with or without ABT, ITZ, and KTZ are shown in Fig. S1A. Furthermore, metabolic rates and inhibition ratios are summarized in Table S1. ABT, ITZ, and KTZ significantly inhibited CYP3A4-mediated MDZ metabolism by rat liver microsomes (Fig. 1A). At 10 μM inhibitor concentration, the rank order of inhibition ratio was as follows: KTZ (94.4 ± 0.8%), ABT (84.6 ± 2.0%), and ITZ (72.6 ± 5.4%). During the metabolism study, ABT and KTZ showed no significant degradation, but ITZ showed slight degradation (Fig. 1B).

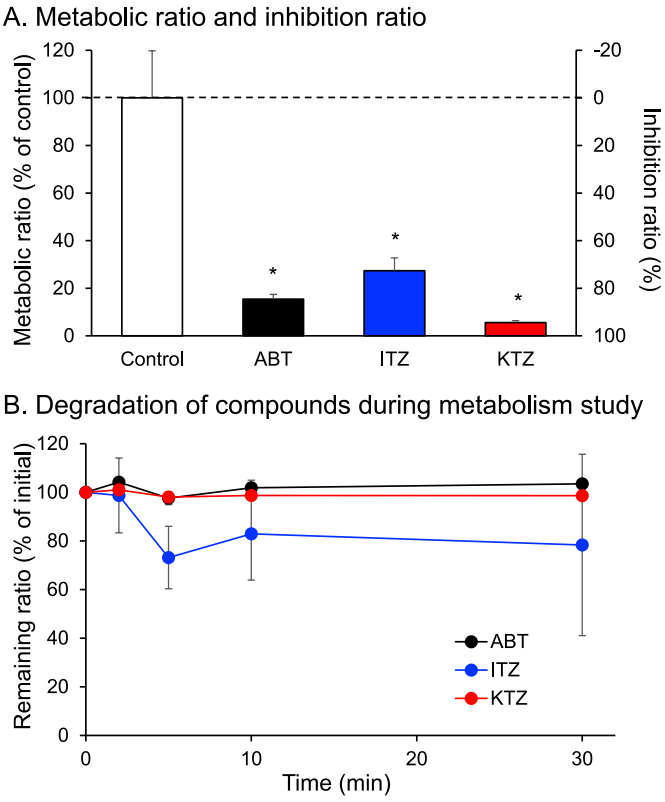

Fig. 1. The inhibition ratio of ABT, ITZ, and KTZ on CYP3A4-mediated MDZ metabolism by rat liver microsome (A) and inhibitor degradation during the inhibition study (B). The remaining inhibitor ratios are indicated relative to time zero. Data are expressed as the mean ± s.d. (n = 4). The mean inhibition ratios of the control, ABT, and KTZ (A) are from *ref*. 17. *Significant difference from the control ($p < 0.05$).

3.2. Effect of newly synthesized compounds on MDZ metabolism and degradation

The time profiles of MDZ metabolism and kinetic parameters are shown in Figs. S1B–C and Table S1, respectively. The inhibition ratio of A-01, A-02, and A-03 was evaluated as 84.7 ± 6.7%, 87.1 ± 2.1%, and 84.3 ± 1.5%, respectively (Fig. 2A). While the amount of A-01 in the test solution did not change during the study, A-02 and A-03 both gradually decreased (Fig. 2B). By the end of the assay, approximately half of the initial amount, before NADPH addition, remained. The inhibition ratios for group B compounds depended markedly on chemical structure (Fig. 3A). No significant inhibitory effects were observed for B-01 (15.5 ± 6.9%), B-04 (39.9 ± 19.9%), and B-08 (10.4 ± 28.8%). B-03, B-05, and B-07 showed moderate inhibitory effects on MDZ metabolism, ranging from 42.6 to 61.8%. MDZ metabolism was strongly inhibited by both B-02 (72.0 ± 5.3%) and B-06 (72.2 ± 19.4%), which is comparable to that of ITZ. Fig. 3B shows the time profile of the compound ratio relative to the initial amount. The concentration of B-01 did not change during the metabolism study; however, that of the other compounds (B-02 to B-08) decreased with time. At 5 min after initiation of the metabolism study the concentrations of compounds B-03, B-04, B-05, and B-08 decreased to less than 20% of the initial concentration. While compounds B-06 and B-07 decreased to approximately 40% 5 min after initiation. Of the B-group esters, the degradation of B-02 was the slowest, indicating that it is the most stable of the B-group esters.

3.3. Hydrolysis study

In the absence of NADPH, the concentrations of IRT and TEM gradually decreased after addition to the test solution containing the rat liver microsomes (Fig. 4A). The concentration of A-01 remained unchanged

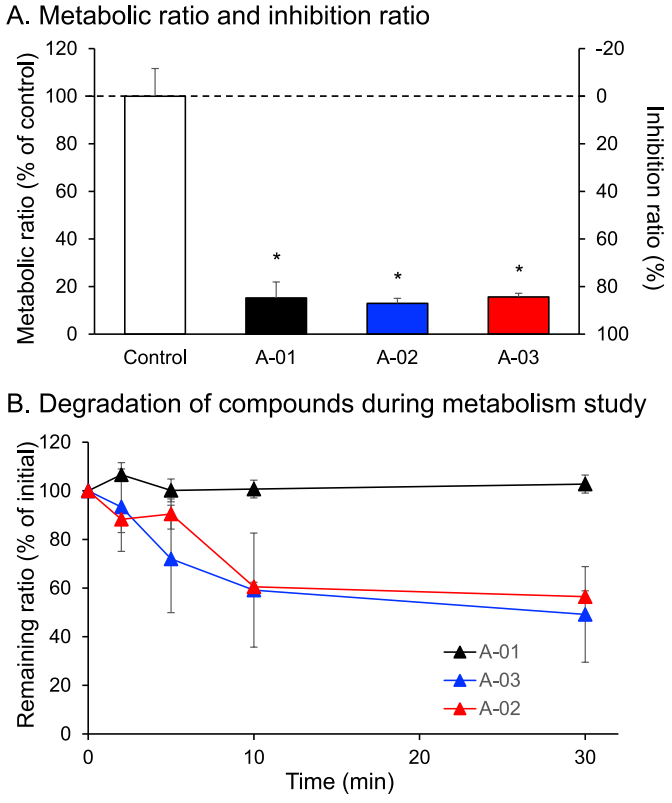

Fig. 2. The inhibition ratio of group A compounds on CYP3A4-mediated MDZ metabolism by rat liver microsome (A) and their degradation during the inhibition study (B). The remaining compound ratios are noted with respect to time zero. Data are expressed as the mean ± s.d. (n = 4). The mean inhibition ratios (A) are from *ref.* 17. *Significant difference from the control ($p < 0.05$).

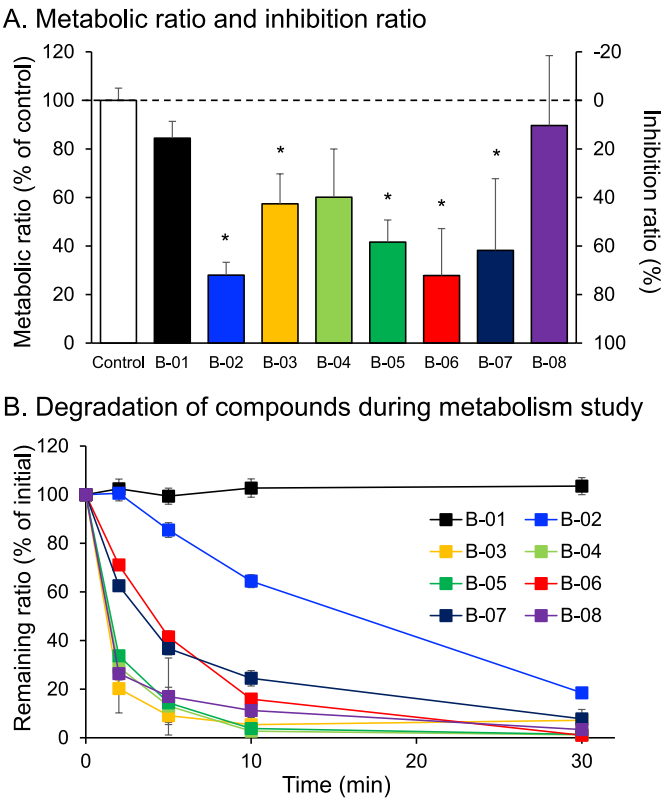

Fig. 3. The inhibition ratio of group B compounds on CYP3A4-mediated MDZ metabolism by rat liver microsome (A) and their degradation during the inhibition study (B). The remaining compound ratios are indicated with respect to the amount at time zero. Data are expressed as the mean ± s.d. (n = 4). The mean inhibition ratios (A) and degradation profile of B-02 (B) are from *ref.* 17. *Significant difference from the control ($p < 0.05$).

during the study. By the 2-min mark, both A-02 and A-03 remained at less than 2% of the initial concentration, indicating that each was immediately degraded by rat liver microsomes after addition (Fig. 4B). The concentration of A-01, derived by A-02 or A-03 hydrolysis, plateaued after 2 min indicating rapid hydrolysis (data not shown). Fig. 4C shows the degradation of compounds B-01, B-02, and B-06. The concentrations of B-02 and B-06 decreased over time, but B-01 remained unchanged. Although the degradation rate of B-06 was faster than that of B-02, both compounds underwent greater than 85% degradation by 30 min. For the studies with B-02 and B-06, the hydrolysate, B-01, gradually increased concentration over time. As a stable mass balance was observed between B-02 and B-01 during the assay, it indicates that B-02 hydrolysis is to B-01 only (Fig. 5). A similar mass balance relation was found for B-06 (data not shown).

3.4. Time-dependent inhibition study

The time profiles of MDZ metabolism and kinetic parameters are shown in Fig. S1D and Table S1, respectively. At time zero, the concentrations of A-02, A-03, B-02, and B-06 were comparable to that of the degradation study at 30 min, indicating that these compounds were primarily degraded during pre-incubation (data not shown). Fig. 6 shows the metabolic and inhibition ratios for the time-dependent inhibition study. The inhibition ratio of ABT was calculated as 90.4 ± 4.6%, comparable to that observed in the metabolism study. Significant inhibition effects for the group A compounds, 70.8 ± 9.7% for A-01, 56.1 ± 7.7% for A-02, and 52.0 ± 21.8% for A-03, were observed. The inhibition of B-01 on MDZ metabolism was not observed for the time-dependent inhibition study. Furthermore, time-dependent inhibition was not observed for compounds B-02 and B-06.

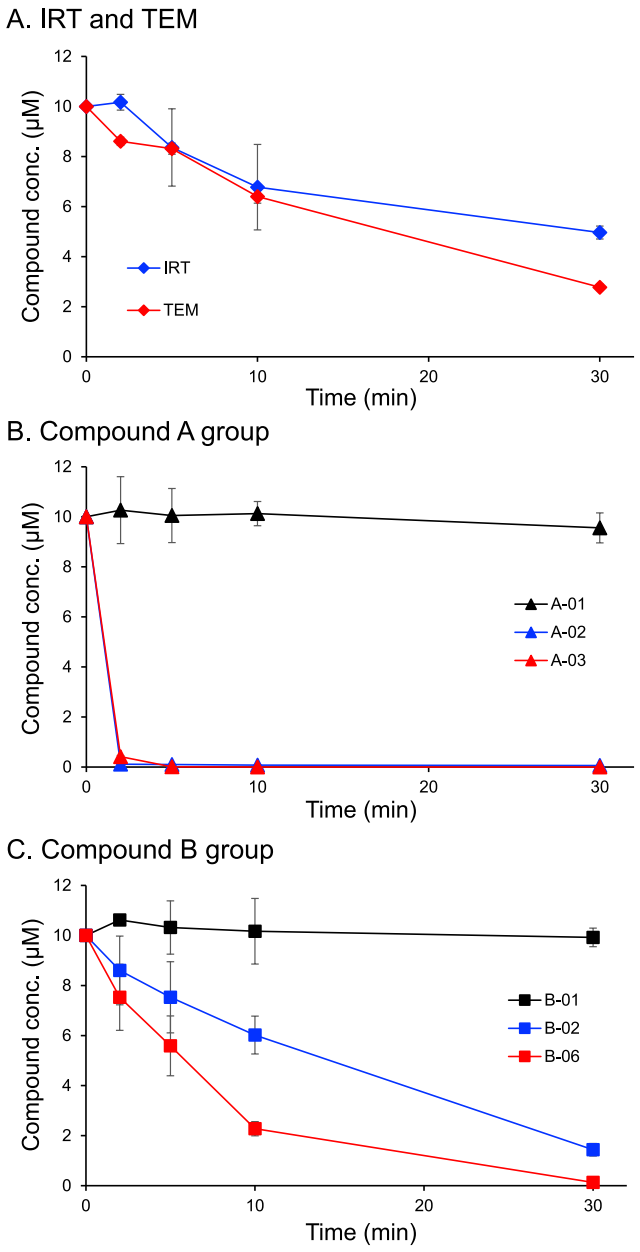

Fig. 4. Hydrolysis time profiles (A; ITR and TEM, B; A-01, A-02, and A-03, C; B-01, B-02, and B-06) from the hydrolysis study. Data are expressed as the mean ± s.d. (n = 3).

4. Discussion

CYP3A4 oxidizes small foreign organic molecules and xenobiotics, such as drugs and toxins. CYP3A4, expressed in the epithelial cells of the small intestine and hepatocytes, influences the first-pass effect of CYP3A4 substrates and hepatic clearance. Therefore, the systemic exposure of CYP3A4 substrates is markedly influenced by the expression level of CYP3A4 and degree of CYP3A4-mediated metabolism inhibition [18–20]. If one compound influences the PK profile of another, they can be respectively referred to as inhibitor and substrate. These interactions can be classified into three major types of enzyme-mediated metabolism inhibition mechanisms. The first mechanism is competitive inhibition, in which the metabolic enzyme metabolizes both the inhibitor and substrate. The second is non-specific inhibition, in the context of CYP3A4 metabolism it usually involves the formation of coordinate bonds between the inhibitor and heme iron, resulting in a loss of affinity for the

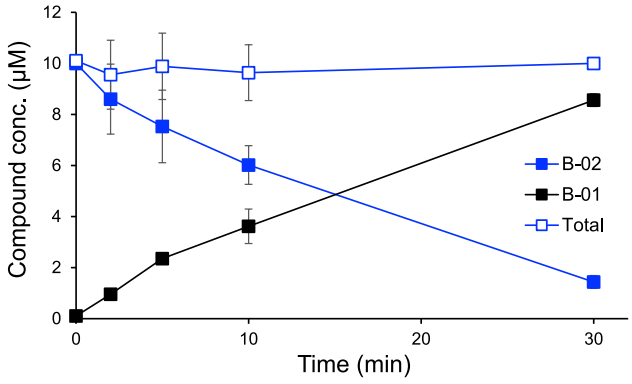

Fig. 5. The mass balance of B-02 during the hydrolysis study. The time profile of B-02 is the same data set shown in Fig. 4. Data are expressed as the mean ± s.d. (n = 3).

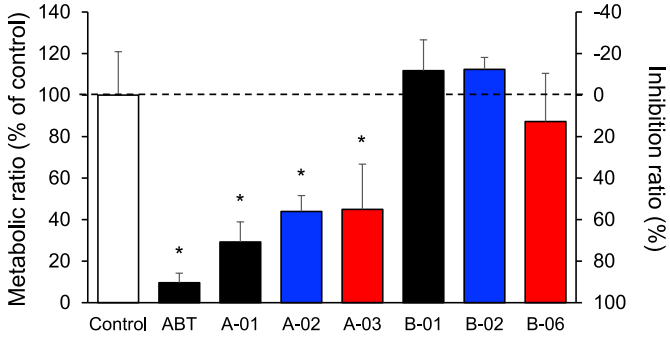

Fig. 6. The inhibition ratios of ABT, A-01, A-02, A-03, B-01, B-02, and B-06 from the time-dependent inhibition study. Data are expressed as the mean ± s.d. (n = 4). *Significant difference from the control ($p < 0.05$).

substrate. However, as this inhibition is reversible, the reduction in plasma concentration over time due to dilution in the body and ultimately excretion of the inhibitor returns the enzymatic activity to normal. The third is mechanism-based inhibition (MBI), in which enzyme-mediated metabolism is halted by the formation of covalent bonds between the enzyme and the active metabolite of the inhibitor, resulting in an irreversible disruption of enzyme metabolism activity [21]. Therefore, subsequent reductions in the plasma concentration of inhibitor does not recover metabolism activity, which is only restored by the replacement of enzyme.

MDZ is a substrate often used *in vitro* and *in vivo* to evaluate the inhibition of CYP3A4-mediated metabolism [22–24] and ABT is a commonly used non-selective CYP inhibitor. Due to the MBI effect for CYP-mediated metabolism [25], ABT significantly inhibits the first-pass effect and drug hepatic clearance [26,27]. KTZ and ITZ show mixed competitive and non-specific inhibitions on CYP3A4-mediated metabolism [28,29]. The imidazole and triazole rings at one terminus of KTZ and ITZ, respectively, are associated with the observed non-specific inhibition. A lone electron pair in the imidazole or triazole ring coordinates to the heme porphyrin iron atom in CYP3A4, resulting in potent inhibition of CYP3A4-mediated metabolism. As both drugs generally act as inhibitors, they are contraindicated with many CYP3A4 substrates in humans [30,31].

In our strategy to enhance the oral availability of CYP3A4 substrates and minimize DDIs with other drugs, a booster with potent inhibition must act transiently upon CYP3A4-mediated metabolism. As MBI induces irreversible CYP3A4-mediated metabolism inhibition, it can no longer be considered effective for this. The goal is to achieve potent and transient inhibition by employing non-specific inhibition and antedrug

characteristics. In this study, an imidazole ring and ester bond were selected as respective active and inactivation sites for potent and transient inhibition. As lipophilicity is an important factor for CYP substrates [32], the high lipophilicity of an imidazole ring and ester initially inhibits CYP-mediated metabolism, with subsequent hydrolysis decreasing this lipophilicity and reducing the degree of inhibition.

Compounds in groups A and B are newly synthesized based on the antedrug strategy (Table 1). A-01 and B-01 each possess imidazole rings at one end and with hydroxyl or carboxyl groups at the opposite end, respectively. The derivatives of A-01 (A-02 and A-03) and B-01 (B-02 to B-08) have ester bonds with different carboxylic acid and alcohol lengths. Thus, some inhibition ratios are reported as averages from the previous study, these values with standard deviations were used to evaluate this study. The inhibition ratios of A-02 and A-03 were similar and comparable to that of ABT (Fig. 2), although significant hydrolysis was observed (Fig. 2B and 4B). The time-dependent inhibition study with the group A compounds yielded a similar effect on MDZ metabolism (Fig. 6). These results are supported by the significant inhibition of CYP3A4-mediated MDZ metabolism by A-01. This effect is attributed to its lipophilicity. The partition coefficient (cLogP) and p*K*a of A-01 were calculated to be 2.9 and 14.3 using ChemDraw, respectively. These physicochemical properties imply a high lipophilicity for A-01 at physiological pH, 7.4. Therefore, A-02 and A-03 did not show antedrug characteristics because the hydrolysates significantly inhibit CYP3A4-mediated MDZ metabolism.

The inhibition by group B compounds showed a strong dependence on chemical structure (Fig. 3). The inhibition and time-dependent inhibition studies indicated that B-01 does not significantly influence MDZ metabolism. The cLogP of B-01 is 3.6 for the unionized state and −0.4 for the ionized state. As the p*K*a of B-01 is estimated to be 4.3, the Henderson-Hasselbalch equation predicts a unionized fraction of less than 0.1%, leading to a low lipophilicity under physiological pH. Hence, the hydrolysate of B-02 to B-08 does not affect MDZ metabolism by CYP3A4. The hydrolysis study with B-01, B-02, and B-06 demonstrated that B-01 ester compounds hydrolyzed over time in a strongly structure-dependent manner (Figs. 4C and 5). Indeed, before initiating the inhibition study, some compounds had already undergone hydrolysis, indicating that ester inhibition ratios are strongly affected by their hydrolysis. Compounds that underwent slow hydrolysis (B-02 and B-06) showed a trend indicating a relatively strong inhibition effect. A longer incubation may easily grasp the real-time change in the metabolic activity as the concentration of B-02 or B-06 decreases. However, the control experiment in the inhibition and time-dependent inhibition studies indicated that the rate of midazolam metabolism reduced with time (Table S1), which could be attributed to a decrease in the activity of microsomes. Hence, the time-dependent inhibition study was performed to assess the change in the inhibition activity by hydrolysis of B-02 and B-06. The inhibition of CYP3A4-mediated MDZ metabolism was completely reversed upon hydrolysis of B-02 and B-06 (Fig. 6). This demonstrated that hydrolysis of B-01 ester compounds eliminates their inhibition activity. The time-dependent inhibition study with B-01 ester compounds suggested that irreversible inhibition, MBI, was not denied an inhibition mechanism. The chemical structure difference between A-01 and B-01 is only in the hydrophilic terminus of the molecules, either a hydroxyl or carboxyl group. Despite the structural similarities, there is a significant difference in inhibition. This implies that the inhibition mechanism for these compounds is non-specific, involving the formation of a coordination bond between the heme iron atom and an imidazole ring electron lone pair. However, the B-01 ester compound inhibition mechanism requires evaluation to demonstrate that these are safe PK boosters. Since B-01 generated in the liver after oral administration of B-01 ester can enter the systemic circulation, additional effects, including toxicity, of B-01 should be assessed in the future study before proceeding to the clinical study. This relates to the third characteristic of a safe booster described in the introduction.

Carboxylesterases (CES) catalyze ester bond hydrolysis which often regulates substrate PK, including prodrugs and antedrugs [33,34]. When considering the first-pass effect, the expression of the CES family and its activity in epithelial cells of the small intestine and hepatocytes impact the hydrolysis of ester bond containing compounds. Various CES are identified in humans [35]; however, the majority of CES expressions identified are CES1 and CES2 [36–38]. Human hepatocytes predominantly contain CES1 with smaller quantities of CES2, whereas the small intestine contains CES2 with virtually no CES1 [39,40]. In this study, the rat liver microsome was used to assess inhibition and time-dependent inhibition effects. Additionally, the CES responsible for the hydrolysis of the tested compounds is unidentified. As CES1 and CES2 are both expressed in the rat liver [41], IRT, a model substrate for CES2, and TEM, a model substrate for CES1, are degraded over time by their respective enzymes (Fig. 4A). As larger acyl groups in the ester compounds show higher affinities to CES1 than CES2 [42], the hydrolysis of compound B group with ester bonds may be catalyzed predominantly by CES1. If so, the esters of B-01 will enable inhibition of intestinal CYP3A-mediated metabolism, with hydrolysis by hepatocytes inducing only slight inhibition. If a newly-developed booster realizes a potent inhibition on CYP3A4-mediated metabolism and high stability against hydrolysis by CES1, the bioavailability of CYP3A4 substrates is expected to be dramatically improved; however, the systemic clearance of CYP3A4 substrates is also significantly reduced for a long time. In our concept, an ideal booster potently inhibits only intestinal CYP3A4 without any inhibition on hepatic CYP3A4. To achieve this goal, an orally-administered safe booster needs to be hydrolyzed not by intestinal CES2, but rapidly by hepatic CES1. Further study is required to confirm which CES is primarily responsible for hydrolysis of the B-01 esters. In this study, rat liver microsomes were used as a model source of CYP3A4 because it was often used to evaluate CYP3A4-mediated metabolism inhibition and the present study aims to demonstrate the antedrug mechanism of our compounds. In addition, rats can be a possible animal for future studies demonstrating the *in vivo* effect. However, these studies require replication with human S9 liver and small intestine fraction to further assess compound viability, along with evaluations of inhibition selectivity on other enzymes such as CYP2C9, CYP2C19.

In conclusion, we demonstrated the significant inhibition of our newly synthesized compounds containing an alcohol ester and imidazole ring on CYP3A4-mediated drug metabolism, and the influence of subsequent hydrolysis which eliminates the induced inhibition. Through this, a potent inhibitory effect on CYP3A-mediated drug metabolism and transient inhibitory mechanism were demonstrated. Future studies will involve further evaluation of *in vivo* efficacies and the antedrug characteristics of B-01 ester compounds.

Author contributions

All authors have read and agree to the published version of the manuscript. Conceptualization, M.K., and K.K.; investigation, S.T., S.F., K.M., and K.K.; methodology, T.M., and K.M.; validation, T.M., K.M., T. T., and K.K.; formal analysis, M.K., and K.K.; writing—original draft preparation, M.K. and K.K.; writing—review and editing, K.M., and T.T.; supervision, M.O., and S.Y.

Conflict of interest

The authors declare no conflict of interest associated with this manuscript.

Acknowledgments

The Mochida Memorial Foundation for Medical and Pharmaceutical Research and the JSPS KAKENHI (23K04969) financially support a part of this study.

Appendix A. Supplementary data

Supplementary data to this article can be found online at https://doi.org/10.1016/j.dmpk.2024.101005.

References

[1] Frank R, Hargreaves R. Clinical biomarkers in drug discovery and development. Nat Rev Drug Discov 2003 Jul;2(7):566–80. https://doi.org/10.1038/nrd1130. PMID: 12838269.

[2] Marsden CD, Barry PE, Parkes JD, Zilkha KJ. Treatment of Parkinson's disease with levodopa combined with L-alpha-methyldopahydrazine, an inhibitor of extracerebral DOPA decarboxylase. J Neurol Neurosurg Psychiatry 1973 Feb;36(1):10–4. https://doi.org/10.1136/jnnp.36.1.10. PMID: 4691682; PMCID: PMC494269.

[3] Reading C, Cole M. Clavulanic acid: a beta-lactamase-inhiting beta-lactam from Streptomyces clavuligerus. Antimicrob Agents Chemother 1977 May;11(5):852–7. https://doi.org/10.1128/AAC.11.5.852. PMID: 879738; PMCID: PMC352086.

[4] Kumar GN, Rodrigues AD, Buko AM, Denissen JF. Cytochrome P450-mediated metabolism of the HIV-1 protease inhibitor ritonavir (ABT-538) in human liver microsomes. J Pharmacol Exp Ther 1996 Apr;277(1):423–31. Erratum in: J Pharmacol Exp Ther 1997 Jun;281(3):1506. PMID: 8613951.

[5] Lee CG, Gottesman MM, Cardarelli CO, Ramachandra M, Jeang KT, Ambudkar SV, et al. HIV-1 protease inhibitors are substrates for the MDR1 multidrug transporter. Biochemistry 1998 Mar 17;37(11):3594–601. https://doi.org/10.1021/bi972709x. PMID: 9530286.

[6] Hsu A, Granneman GR, Bertz RJ. Ritonavir. Clinical pharmacokinetics and interactions with other anti-HIV agents. Clin Pharmacokinet 1998 Oct;35(4):275–91. https://doi.org/10.2165/00003088-199835040-00002. Erratum in: Clin Pharmacokinet 1998 Dec;35(6):473. PMID: 9812178.

[7] Bartlett JA, Fath MJ, Demasi R, Hermes A, Quinn J, Mondou E, et al. An updated systematic overview of triple combination therapy in antiretroviral-naive HIV-infected adults. AIDS 2006 Oct 24;20(16):2051–64. https://doi.org/10.1097/01.aids.0000247578.08449.ff. PMID: 17053351.

[8] Martinez-Cajas JL, Wainberg MA. Protease inhibitor resistance in HIV-infected patients: molecular and clinical perspectives. Antiviral Res 2007 Dec;76(3):203–21. https://doi.org/10.1016/j.antiviral.2007.06.010. Epub 2007 Jul 16. PMID: 17673305.

[9] Menon RM, Klein CE, Podsadecki TJ, Chiu YL, Dutta S, Awni WM. Pharmacokinetics and tolerability of paritaprevir, a direct acting antiviral agent for hepatitis C virus treatment, with and without ritonavir in healthy volunteers. Br J Clin Pharmacol 2016 May;81(5):929–40. https://doi.org/10.1111/bcp.12873. Epub 2016 Feb 24. PMID: 26710243; PMCID: PMC4834602.

[10] Ritonavir-boosted nirmatrelvir (Paxlovid). package insert. Food and Drug Administration; 2023. Available at: https://www.accessdata.fda.gov/drugsatfda_docs/label/2023/217188s000lbl.pdf. [Accessed 10 November 2023].

[11] Food and Drug Administration. Fact sheet for healthcare providers: Emergency Use Authorization for Paxlovid. 2023. Available at: . [Accessed 10 November 2023].

[12] Kirby BJ, Collier AC, Kharasch ED, Whittington D, Thummel KE, Unadkat JD. Complex drug interactions of HIV protease inhibitors 1: inactivation, induction, and inhibition of cytochrome P450 3A by ritonavir or nelfinavir. Drug Metab Dispos 2011 Jun;39(6):1070–8. https://doi.org/10.1124/dmd.110.037523. Epub 2011 Mar 15. PMID: 21406602; PMCID: PMC3100903.

[13] Kageyama M, Namiki H, Fukushima H, Terasaka S, Togawa T, Tanaka A, et al. Effect of chronic administration of ritonavir on function of cytochrome P450 3A and P-glycoprotein in rats. Biol Pharm Bull 2005 Jan;28(1):130–7. https://doi.org/10.1248/bpb.28.130. PMID: 15635177.

[14] Ramanathan S, Mathias AA, German P, Kearney BP. Clinical pharmacokinetic and pharmacodynamic profile of the HIV integrase inhibitor elvitegravir. Clin Pharmacokinet 2011 Apr;50(4):229–44. https://doi.org/10.2165/11584570-000000000-00000. PMID: 21348537.

[15] Tseng A, Hughes CA, Wu J, Seet J, Phillips EJ. Cobicistat versus ritonavir: similar pharmacokinetic Enhancers but some important differences. Ann Pharmacother 2017 Nov;51(11):1008–22. https://doi.org/10.1177/1060028017717018. Epub 2017 Jun 19. PMID: 28627229; PMCID: PMC5702580.

[16] Xu L, Liu H, Murray BP, Callebaut C, Lee MS, Hong A, et al. Cobicistat (GS-9350): a potent and selective inhibitor of human CYP3A as a novel Pharmacoenhancer. ACS Med Chem Lett 2010 May 17;1(5):209–13. https://doi.org/10.1021/ml1000257. PMID: 24900196; PMCID: PMC4007915.

[17] Kawai K, Okada J, Nakae M, Tsujimura T, Karuo Y, Tarui A, et al. Discovery of benzyloxyphenyl- and phenethylphenyl-imidazole derivatives as a new class of ante-drug type boosters. Bioorg Med Chem Lett 2022 Sep 15;72:128868. https://doi.org/10.1016/j.bmcl.2022.128868. Epub 2022 Jun 25. PMID: 35764276.

[18] Gupta N, Hanley MJ, Venkatakrishnan K, Bessudo A, Rasco DW, Sharma S, et al. Effects of strong CYP3A inhibition and induction on the pharmacokinetics of Ixazomib, an oral proteasome inhibitor: results of drug-drug interaction studies in patients with Advanced Solid Tumors or Lymphoma and a physiologically based pharmacokinetic analysis. J Clin Pharmacol 2018 Feb;58(2):180–92. https://doi.org/10.1002/jcph.988. Epub 2017 Aug 11. PMID: 28800141; PMCID: PMC5811830.

[19] Cotreau MM, Siebers NM, Miller J, Strahs AL, Slichenmyer W. Effects of ketoconazole or rifampin on the pharmacokinetics of tivozanib hydrochloride, a vascular endothelial growth factor receptor tyrosine kinase inhibitor. Clin Pharmacol Drug Dev 2015 Mar;4(2):137–42. https://doi.org/10.1002/cpdd.145. Epub 2014 Oct 1. PMID: 27128217.

[20] Jalava KM, Olkkola KT, Neuvonen PJ. Itraconazole greatly increases plasma concentrations and effects of felodipine. Clin Pharmacol Ther 1997 Apr;61(4):410–5. https://doi.org/10.1016/S0009-9236(97)90191-0. PMID: 9129558.

[21] Deodhar M, Al Rihani SB, Arwood MJ, Darakjian L, Dow P, Turgeon J, et al. Mechanisms of CYP450 inhibition: Understanding drug-drug interactions due to mechanism-based inhibition in clinical Practice. Pharmaceutics 2020 Sep 4;12(9):846. https://doi.org/10.3390/pharmaceutics12090846. PMID: 32899642; PMCID: PMC7557591.

[22] Kashiwabuchi Y, Nishimura Y, Kurata N, Iwase M, Kiuchi Y, Nobe K. Inhibition of CYP3A-mediated midazolam metabolism by Kaempferia Parviflora. Food Saf (Tokyo) 2022 Mar 3;10(1):32–41. https://doi.org/10.14252/foodsafetyfscj.D-21-00013. PMID: 35510070; PMCID: PMC9008879.

[23] Luo X, Li XM, Hu ZY, Cheng ZN. Evaluation of CYP3A activity in humans using three different parameters based on endogenous cortisol metabolism. Acta Pharmacol Sin 2009 Sep;30(9):1323–9. https://doi.org/10.1038/aps.2009.116. Epub 2009 Aug 24. PMID: 19701237; PMCID: PMC4007188.

[24] Kanazu T, Yamaguchi Y, Okamura N, Baba T, Koike M. Model for the drug-drug interaction responsible for CYP3A enzyme inhibition. II: establishment and evaluation of dexamethasone-pretreated female rats. Xenobiotica 2004 May;34(5):403–13. https://doi.org/10.1080/00498250410001685746. PMID: 15370957.

[25] de Montellano PRO. 1-Aminobenzotriazole: a mechanism-based cytochrome P450 inhibitor and Probe of cytochrome P450 Biology. Med Chem 2018;8(3):38. https://doi.org/10.4172/2161-0444.1000495. Epub 2018 Mar 31. PMID: 30221034; PMCID: PMC6137267.

[26] Strelevitz TJ, Foti RS, Fisher MB. In vivo use of the P450 inactivator 1-amino-benzotriazole in the rat: varied dosing route to elucidate gut and liver contributions to first-pass and systemic clearance. J Pharm Sci 2006 Jun;95(6):1334–41. https://doi.org/10.1002/jps.20538. PMID: 16625658.

[27] Kataoka M, Kojima C, Ueda K, Minami K, Higashino H, Sakuma S, et al. Quantitative analysis of pharmacokinetic profiles of verapamil and drug-drug interactions induced by a CYP inhibitor using a stable isotope-labeled compound. Drug Metab Pharmacokinet 2016 Dec;31(6):405–10. https://doi.org/10.1016/j.dmpk.2016.08.001. Epub 2016 Aug 18. PMID: 27876352.

[28] Greenblatt DJ, Zhao Y, Venkatakrishnan K, Duan SX, Harmatz JS, Parent SJ, et al. Mechanism of cytochrome P450-3A inhibition by ketoconazole. J Pharm Pharmacol 2011 Feb;63(2):214–21. https://doi.org/10.1111/j.2042-7158.2010.01202.x. PMID: 21235585.

[29] Wang L, Wu F, Xu J, Wang Y, Fei W, Jiang H, et al. Differential effects of ketoconazole, fluconazole, and itraconazole on the pharmacokinetics of pyrotinib in vitro and in vivo. Front Pharmacol 2022 Sep 7;13:962731. https://doi.org/10.3389/fphar.2022.962731. PMID: 36160438; PMCID: PMC9490176.

[30] NIZORAL® (ketoconazole) Tablets (Janssen pharmaceuticals, Inc., Titusville, NJ). Available at:https://www.accessdata.fda.gov/drugsatfda_docs/label/2013/018533s040lbl.pdf(Accessed on November 10, 2023).

[31] SPORANOX® (itraconazole) Capsules (Janssen pharmaceuticals, Inc., Titusville, NJ). Available at:https://www.accessdata.fda.gov/drugsatfda_docs/label/2010/020083s046lbl.pdf(Accessed on November 10, 2023).

[32] Lewis DF, Jacobs MN, Dickins M. Compound lipophilicity for substrate binding to human P450s in drug metabolism. Drug Discov Today 2004 Jun 15;9(12):530–7. https://doi.org/10.1016/S1359-6446(04)03115-0. PMID: 15183161.

[33] Taketani M, Shii M, Ohura K, Ninomiya S, Imai T. Carboxylesterase in the liver and small intestine of experimental animals and human. Life Sci 2007 Aug 23;81(11):924–32. https://doi.org/10.1016/j.lfs.2007.07.026. Epub 2007 Aug 10. PMID: 17764701.

[34] Hatfield MJ, Tsurkan L, Garrett M, Shaver TM, Hyatt JL, Edwards CC, et al. Organ-specific carboxylesterase profiling identifies the small intestine and kidney as major contributors of activation of the anticancer prodrug CPT-11. Biochem Pharmacol 2011 Jan 1;81(1):24–31. https://doi.org/10.1016/j.bcp.2010.09.001. Epub 2010 Sep 15. PMID: 20833148; PMCID: PMC2991631.

[35] Holmes RS, Cox LA, VandeBerg JL. Mammalian carboxylesterase 3: comparative genomics and proteomics. Genetica 2010 Jul;138(7):695–708. https://doi.org/10.1007/s10709-010-9438-z. Epub 2010 Apr 28. PMID: 20422440; PMCID: PMC2896070.

[36] Satoh T, Hosokawa M. The mammalian carboxylesterases: from molecules to functions. Annu Rev Pharmacol Toxicol 1998;38:257–88. https://doi.org/10.1146/annurev.pharmtox.38.1.257. PMID: 9597156.

[37] Hosokawa M, Furihata T, Yaginuma Y, Yamamoto N, Koyano N, Fujii A, et al. Genomic structure and transcriptional regulation of the rat, mouse, and human carboxylesterase genes. Drug Metab Rev 2007;39(1):1–15. https://doi.org/10.1080/03602530600952164. PMID: 17364878.

[38] Satoh T, Hosokawa M. Structure, function and regulation of carboxylesterases. Chem Biol Interact 2006 Sep 25;162(3):195–211. https://doi.org/10.1016/j.cbi.2006.07.001. Epub 2006 Jul 6. PMID: 16919614.

[39] Imai T, Taketani M, Shii M, Hosokawa M, Chiba K. Substrate specificity of carboxylesterase isozymes and their contribution to hydrolase activity in human liver and small intestine. Drug Metab Dispos 2006 Oct;34(10):1734–41. https://doi.org/10.1124/dmd.106.009381. Epub 2006 Jul 12. PMID: 16837570.

[40] Zhang W, Xu G, McLeod HL. Comprehensive evaluation of carboxylesterase-2 expression in normal human tissues using tissue array analysis. Appl Immunohistochem Mol Morphol 2002 Dec;10(4):374–80. https://doi.org/10.1097/00129039-200212000-00015. PMID: 12607608.